On the correlation between the self-organized island pattern and substrate elastic anisotropy

E. Pan[a] and R. Zhu
Department of Civil Engineering, University of Akron, Akron, Ohio 44325

P. W. Chung
U.S. Army Research Laboratory, Aberdeen Proving Ground, Maryland 21005

(Received 1 February 2006; accepted 6 May 2006; published online 13 July 2006)

Self-organized quantum dots pattern depends strongly on the elastic strain energy of the substrate. It is well-known experimentally that for the elastic substrate with a high degree of anisotropy, the epitaxially grown island patterns are different for different growth orientations. In this paper, by incorporating the anisotropic strain energy field into a kinetic Monte Carlo algorithm for adatom diffusion, we show that the self-organized island pattern on the surface of an anisotropic substrate is closely correlated to the elastic energy distribution on the surface. The anisotropic substrates studied are GaAs with different growth orientations (001), (111), and (113). An isotropic substrate Iso (001), reduced from GaAs, is also investigated for the purpose of comparison. The island patterns on these substrates with and without elastic strain energy are presented. Besides the effect of substrate anisotropy, different growth parameters, including temperature, coverage, and interruption time, are further investigated to identify the optimal growth values. It is observed that the strain energy field in the substrate is the key factor that controls the island pattern, and that the latter is closely correlated to the substrate orientation (anisotropy). Our simulated patterns are also in qualitative agreement with recent experimental growth results. © *2006 American Institute of Physics*. [DOI: 10.1063/1.2213153]

I. INTRODUCTION

The fabrication of semiconductor nanostructures has attracted considerable interest in recent years due to their wide-range applications in optoelectronics and semiconductor devices. Among many other techniques, the direct growth of nanostructures has evolved as a promising approach to achieve devices.[1–3] Usually, the thin film layer has different material property as compared to the substrate material, and thus such structures are generally known as heterostructures. Due to the difference in material property and hence the difference in the lattice parameter, lattice-misfit induced strains occur and thus the thin layer deposited on the substrate will break up into coherently strained islands to release some of the strain energy. During epitaxial growth, a strained film can relax its strain by one of the following three mechanisms: (1) formation of dislocation, (2) surface roughening, and (3) cracking. The second mechanism, also called the Stranski-Krastanov growth mode, has attracted significant attention due to its potential as a technique to manufacture self-organized quantum-dot (QD) and quantum-wire structures.[4] The driving mechanism for this growth mode transition is the very efficient strain energy relaxation.

In self-organized QD island research, both theoretical[5,6] and experimental[7–12] studies have shown that the interaction among islands via their elastic strain fields[13,14] may lead to a gradual improvement in size homogeneity, as well as to a more uniform lateral island spacing. Holy *et al.* have further shown that the vertical and lateral correlations in self-organized QD superlattices can be explained by taking into account the elastic anisotropy of the materials.[10] In these superlattices, dot correlations are induced by the interaction among dots via their elastic strain fields. Above the buried islands, the elastic energy distribution on the surface exhibits pronounced minima and maxima in the lateral directions. Many continuum mechanics approaches, including the finite element analysis and Fourier transformation method, were proposed to study the effect of elastic anisotropy on the lattice-misfit induced strain energy field.[15–17] While the continuum mechanics approaches reveal various interesting features showing the direct role of elastic anisotropy on the self-organized growth pattern,[17,18] they fail to connect the growth ordering and pattern to the growth parameters, a serious drawback in the continuum mechanics analysis. Furthermore, the identification of a set of optimal growth parameters would be most useful to experimentalists.

The kinetic Monte Carlo (KMC) has been proposed recently to study QD island self-organization by many researchers[19–24] where the growth parameters are directly involved in the simulation.[25] It has been shown that the main growth parameters affecting QD island distribution patterns are the temperature T, flux rate F to the surface during deposition, surface coverage c, and growth interruption time t_i.[21,25] Based on a proposed coupled KMC, the authors simulated the island ordering and narrow size distribution in two dimensions and further identified a set of optimal growth parameters for the assumed model system.[25] However, how the substrate anisotropy (or orientation) affects the island

[a]Electronic mail: pan2@uakron.edu

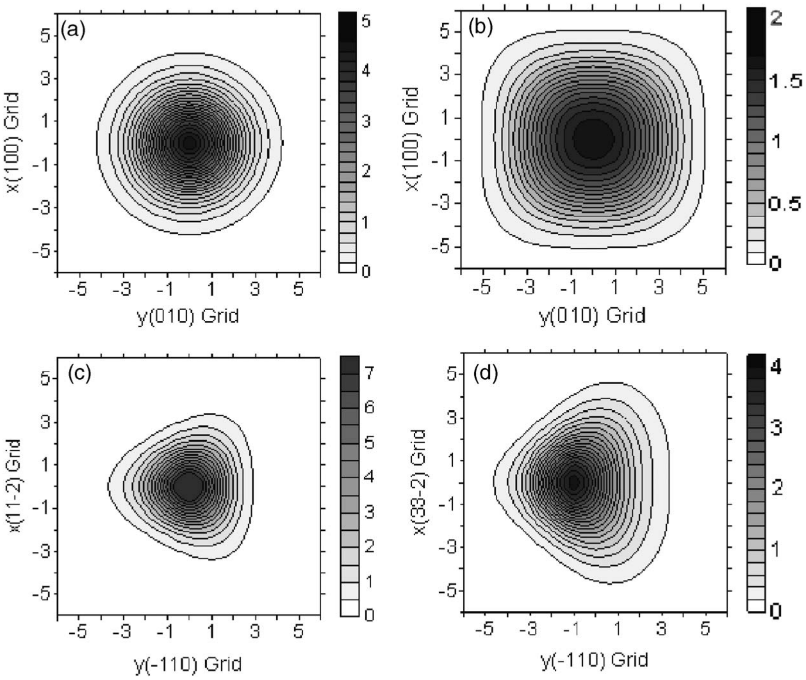

FIG. 1. Contours of the normalized elastic strain energy distribution on the substrate surface of isotropic Iso(001) (a), and anisotropic GaAs(001) (b), GaAs(111) (c), and GaAs (113) (d).

pattern has not been studied so far within the coupled KMC algorithm where the long-range strain energy field is included.

Therefore, in this paper, we apply the coupled KMC self-organization model to study the effect of elastic anisotropy on the QD island lateral ordering and pattern [a two-dimensional (2D) model only]. In our simulation, the atom hopping rate is governed by the Arrenius law which is enhanced by the long-range strain energy field due to the lattice-misfit strain. The induced elastic strain field is obtained using the Green's function solution for the anisotropic semiconductor substrate developed recently.[26,27] Besides the isotropic substrate model Iso (001), three anisotropic substrates derived from GaAs were included, i.e., GaAs (001), GaAs (111) and GaAs (113). Different growth parameters, namely, temperature T, coverage c, and interruption time t_i, are also discussed. While results with different growth parameters demonstrate that temperature, coverage, and interruption time affect the average island size and number of atoms within each island, our simulations further clearly indicate the close correlation between the substrate orientation (elastic anisotropy) and the growth pattern, which also qualitatively agree with recent experimental results obtained via scanning tunneling microscopy (STM).[28,29]

II. SELF-ORGANIZED ORDERING AND PATTERN

In our coupled KMC simulation, the lattice-misfit induced strain energy is added to the Arrenius law to accurately account for the effect of the long-range strain field on the growth patterns. We choose the substrate to be GaAs, and consequently, the lattice-misfit strain is hydrostatic, i.e., $\gamma_{ij}^* = \gamma^* \delta_{ij}$ with $\gamma^* = 0.07$. The nonzero elastic coefficients for GaAs (001) (Ref. 26) are taken to be $C_{11} = 118.8 \times 10^9\ \mathrm{N/m^2}$, $C_{12} = 53.8 \times 10^9\ \mathrm{N/m^2}$, and $C_{44} = 59.4 \times 10^9\ \mathrm{N/m^2}$, when the growth is along the (001) direction. For the substrate with growth along the (111) and (113) directions, the elastic moduli of GaAs (111) and GaAs (113) are transformed from GaAs (001).[27] An isotropic substrate model, called Iso (001), is also introduced for the purpose of comparison in which the elastic constants of GaAs (001) are replaced with the corresponding isotropic constants.[30] In other words, in the isotropic Iso (001) model, the elastic constants C_{12} and C_{44} are the same as those of GaAs (001), i.e., $C_{12} = 53.8 \times 10^9\ \mathrm{N/m^2}$ and $C_{44} = 59.4 \times 10^9\ \mathrm{N/m^2}$, with $C_{11} = 172.6 \times 10^9\ \mathrm{N/m^2}$ obtained by imposing the isotropic condition $C_{11} - C_{12} - 2C_{44} = 0$.[30] For the sake of easy reference, all the elastic coefficient matrices are given in the Appendix.

Once we have defined the substrate, we then use our coupled KMC to model the deposition and diffusion processes. Under different growth parameters (deposition rate F, temperature T, coverage c, and interruption time t_i) we simulate the adatom growth behavior over a grid of 200×200 on the surface of the substrate. We remark that in this article, only the in-plane or the so-called two-dimensional growth is considered.

We further point out that, due to its rapid decay behavior, the strain energy field is not evaluated over the whole problem domain but rather only over a circular area of a given radius (e.g., thirty grids[25]) around the source point. This decay feature can be observed from Fig. 1 where the elastic strain energy field E_{str} on the surface of substrates Iso (001), GaAs (001), GaAs (111), and GaAs (113) due to a buried island is plotted. Furthermore, Fig. 1 also shows clearly the direct correlation between the strain energy contour shape and the substrate orientation. The different strain energy patterns on the surface of Iso (001), GaAs (001), GaAs (111), and GaAs (113) will result in different island distributions/patterns, as we will discuss below using our coupled KMC simulation.

Shown in Figs. 2(a)–2(d) are the island orderings and patterns of the adatoms on the surface of substrates Iso (001),

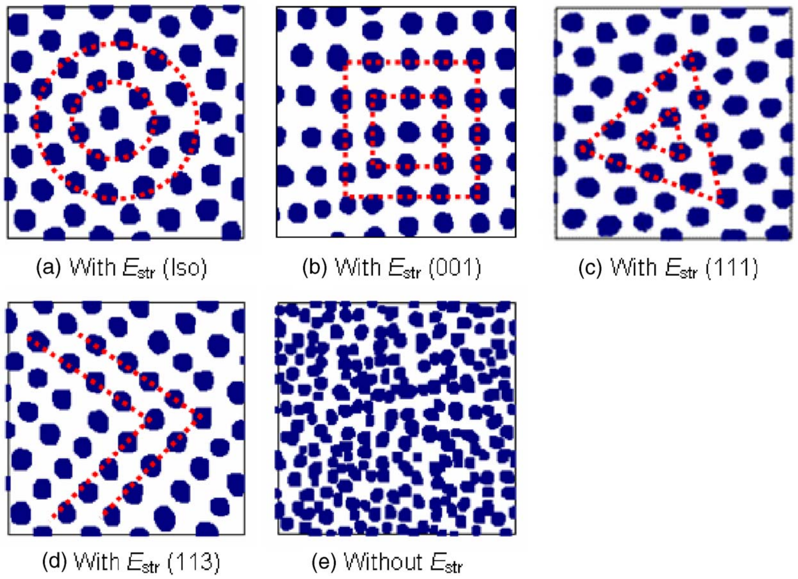

FIG. 2. (Color online) Island ordering and pattern on the surface of GaAs with strain energy E_{str} of Iso (001) (a), with anisotropic strain energy E_{str} of GaAs (001) (b), GaAs (111) (c), and GaAs (113) (d). The island ordering and pattern on the surface of GaAs without strain energy E_{str} is shown in (e) for comparison. Different island orderings and patterns (red dashed lines) corresponding to the GaAs substrate with different growth orientations can be clearly observed from (a) to (d), which can be further compared to the elastic strain energy in Fig. 1. Other simulation parameters are $T=750$ K, $F=1.0$ Ml/s, $c=20\%$, and $t_i=200$ s, on a grid of 200×200.

GaAs (001), GaAs (111), and GaAs (113), respectively. The simulation parameters are temperature $T=750$ K, flux rate $F=1.0$ Ml/s, surface coverage $c=20\%$, and interruption time $t_i=200$ s. It is obvious that different substrate orientations result in different growth patterns, due mainly to the different strain energy patterns on the surface of the substrate (Fig. 1). Furthermore, without consideration of the lattice-misfit induced strain energy, neither uniform size nor ordered spatial ordering can be observed [Fig. 2(e)] and one would therefore expect Ostwald ripening.[31,32]

In order to show the island distribution more clearly, we plot the island density distribution in Fig. 3 where the number of adatoms per unit area is used as the height. From Fig. 3, we observe again that without strain energy, randomly ordered islands [Fig. 3(e)] are usually formed and often associated with Ostwald ripening;[32] however, with the strain energy E_{str}, isolated and ordered islands (for both size and distribution) can be observed [Figs. 3(a)–3(d)]. Furthermore, different island patterns are correlated closely to different growth orientations [GaAs (001), GaAs (111), and GaAs (113) to Figs. 3(b)–3(d)], with the latter corresponding to the different strain energy distributions as shown in Fig. 1. These results indicate that the long-range strain energy could be one of the very important factors controlling the ordered island size and pattern. Actually, images of the island patterns on different anisotropic substrates from experiments have also shown that a direct correlation exists between the island pattern and substrate anisotropy (or growth orientation), as recently presented by Jacobi[33] where InAs QDs were grown on GaAs (001) and GaAs (113) substrates and by Brune *et al.*[28,29] where the influence of the elastic strain on Ag self-diffusion and nucleation was investigated.

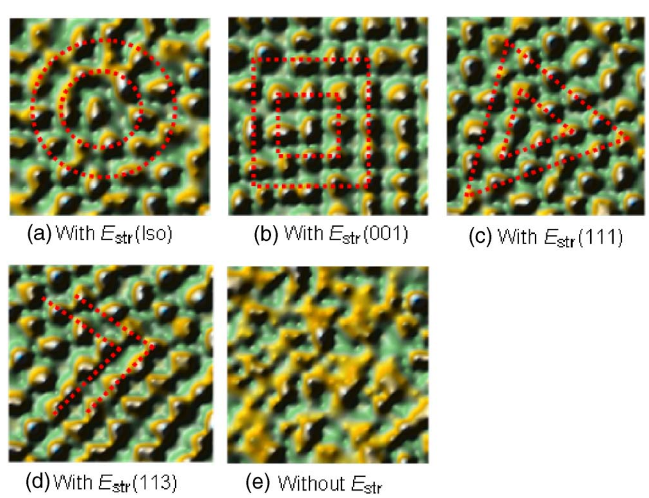

FIG. 3. (Color online) Three-dimensional island density distribution where the height is proportional to the number of adatoms per unit area: on the surface of GaAs with strain energy E_{str} of Iso (001) (a), with anisotropic strain energy E_{str} of GaAs (001) (b), GaAs (111) (c), and GaAs (113) (d). Different island orderings and patterns (red dashed lines) corresponding to different growth orientations can be clearly observed, which can be further compared to the elastic strain energy in Fig. 1. Shown in (e) is the island density distribution on the GaAs substrate without strain energy E_{str}. Other simulation parameters are $T=750$ K, $F=1.0$ Ml/s, $c=20\%$, and $t_i=200$ s, on a grid of 200×200.

III. EFFECT OF DIFFERENT GROWTH PARAMETERS

In our previous paper,[25] we studied the effect of growth parameters (temperature, flux rate, coverage, and interruption time) and showed some typical island patterns for different growth parameters. In that paper, however, no discussion is given on the effect of substrate anisotropy (or orientation) on the growth pattern. Therefore, in what follows, we investigate the effect of the growth parameters on the number of islands and average size of the islands. Again, we use the four different substrates in our simulation: the isotropic substrate Iso (001) and three anisotropic GaAs substrates with different growth directions, namely, GaAs (001), GaAs (111), and GaAs (113). For all the examples below, the grid size is 200×200 and the strain energy is included. We discuss our results for the temperature, coverage, and interruption time separately. The effect of flux rate on the island size was discussed in our previous paper where it was identified that a small size island distribution usually corresponds to a high flux rate and a large size island distribution to a low flux rate.[25]

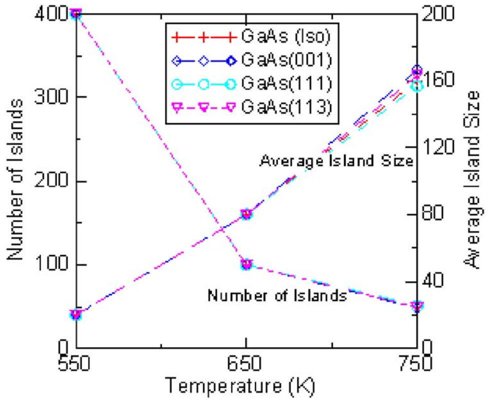

FIG. 4. (Color online) Number of islands and average island size vs temperature for island growth on substrates with different orientations for short temperature range (550–750 K). Other simulation parameters are fixed: $F=1.0$ Ml/s, $c=20\%$, and $t_i=200$ s.

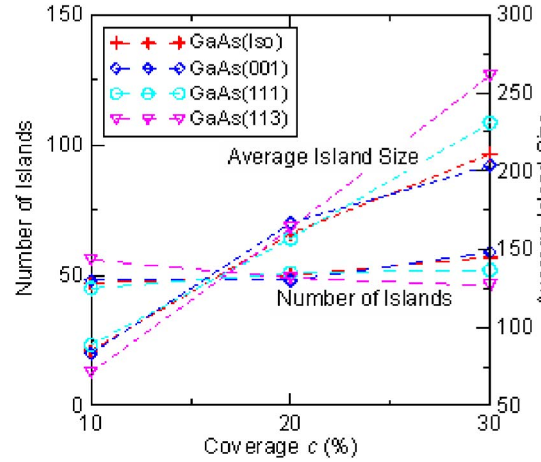

FIG. 6. (Color online) Number of islands and average island size vs coverage for island growth on substrates with different orientations. Other simulation parameters are fixed: $T=750$ K, $F=1.0$ Ml/s, and $t_i=200$ s.

Figures 4 and 5 show the variation of the number of islands and average island size versus temperature. Other fixed growth parameters are flux rate $F=1$ Ml/s, coverage $c=20\%$, and interruption time $t_i=200$ s. We observed from Fig. 4 that, under given growth conditions, the number of islands and average island size are insensitive to the substrate anisotropy (or growth orientation). For all the substrates, with increasing temperature to 750 K, the island size increases and the number of islands decrease. In our previous discussion, we further identified by looking at the island size ordering and distribution that the optimal temperature was around 750 K.[25] The island distribution could be still irregular if temperature is too low (below this critical value) and be unstable if temperature is too high (above this critical value).[25] Therefore, only around the optimized temperature (i.e., $T=750$ K) can one clearly observe ordered and regular island distribution. To further confirm our previous observation, we show here also the variation of the average island size and number of islands versus temperature for a large temperature range [Fig. 5 for GaAs (001) only]. It is observed from Fig. 5 that the average size of the island reaches a maximum at $T=750$ K where the number of islands reaches a minimum.

Figure 6 shows the variation of the number of islands and average island size on the surface of substrates Iso (001), GaAs (001), GaAs (111), and GaAs (113) for different coverages c. The other fixed parameters are temperature $T=750$ K, flux rate $F=1$ Ml/s, and interruption time $t_i=200$ s. It is interesting that with increasing coverage, while the number of islands in the grid is nearly a constant value (around 50), the average island size increases, with GaAs (113) having the largest value followed by GaAs (111). The average island size on the surface of the substrate GaAs (001) has the smallest value.

Finally, Fig. 7 shows the effect of the growth interruption time t_i on the number of islands and average island size. The fixed growth parameters are $T=750$ K, $F=1.0$ Ml/s, and $c=20\%$. It is observed clearly from Fig. 7 that, with increasing interruption time, the number of islands decreases while the average island size increases. Furthermore, at large interruption time ($t_i=200$ s for our case), while the number of islands is nearly the same for different substrate orientations

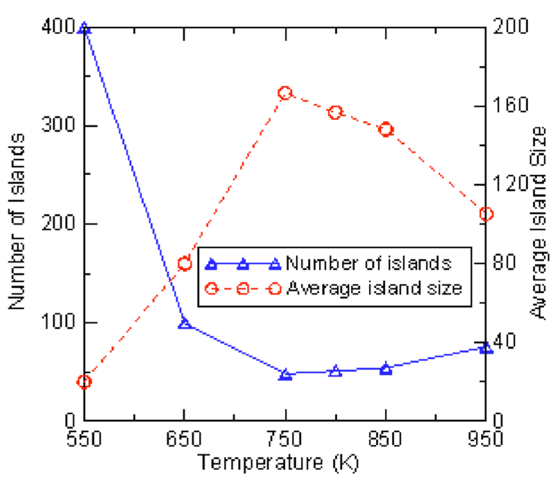

FIG. 5. (Color online) Number of islands and average island size vs temperature for island growth on substrate GaAs (001) for long temperature range (550–950 K). Other simulation parameters are fixed: $F=1.0$ Ml/s, $c=20\%$, and $t_i=200$ s.

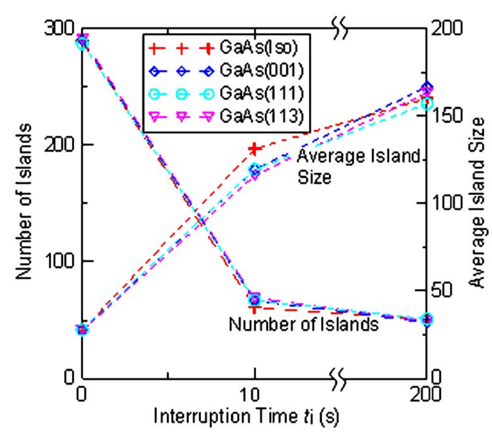

FIG. 7. Number of islands and average island size vs interruption time for island growth on substrates with different orientations. Other simulation parameters are fixed: $T=750$ K, $F=1.0$ Ml/s, and $c=20\%$.

(or different material anisotropies), different substrate orientations predict slightly different island sizes with GaAs (111) having the smallest size among all the substrates.

IV. CONCLUSIONS

In this paper, a coupled kinetic Monte Carlo algorithm is proposed to simulate the growth of adatom islands on the surface of isotropic and anisotropic substrates. The substrates considered are isotropic Iso (001) and anisotropic substrates GaAs (001), GaAs (111), and GaAs (113). The unique feature associated with our coupled KMC is the correct incorporation of the lattice-misfit induced strain energy into the diffusion process governed by the Arrenius law. Our simulation results are consistent with previous experimental observations which show clearly that the growth parameters (temperature, coverage, and interruption time) are important parameters in controlling the island size/distribution. Our results also show that without considering the strain energy, only randomly ordered islands can be formed, which is controlled by the nearest and next nearest binding energy among the adatoms and substrate atoms. When the strain energy field is included, however, isolated and ordered island patterns (both in size and distribution) can be observed. Furthermore, our simulation for self-organized island growth on the surface of the isotropic Iso (001) and anisotropic GaAs (001), GaAs (111), and GaAs (113) indicates that the growth pattern is closely correlated to the substrate anisotropy (or substrate orientation).

ACKNOWLEDGMENT

The authors are grateful for the support provided by ARO.

APPENDIX: ELASTIC COEFFICIENTS OF SUBSTRATES ISO (001), GAAS (001), GAAS (111), AND GAAS (113)

An elastic isotropic model, called Iso (001) is used for the purpose of comparison in which the elastic coefficients of GaAs (001) are made isotropic ($C_{11}-C_{12}-2C_{44}=0$).[30] For the GaAs (111) model, the substrate coordinates are such that the x axis is along $[11-2]$, y axis along $[-110]$, and z axis along $[111]$, while for the GaAs (113) model, the x axis is along $[33-2]$, y axis along $[-110]$, and z axis along $[113]$. The global material properties of GaAs (111) and GaAs (113) are obtained by the well-known tensor transformation[34] from GaAs (001). The inclined material property is obtained by two transformations. For GaAs (111), we first anticlockwise rotate xy plane around z axis by $\pi/4$ (view from positive z axis); then we anticlockwise rotate the new xz-plane around the new y axis by $\pi/2-\cos^{-1}(\sqrt{2/3})$ (view from positive new y axis). Similarly, for GaAs (113), we first anticlockwise rotate xy plane around z axis by $\pi/4$ (view from positive z axis); then we anticlockwise rotate the new xz plane around the new y axis by $\tan^{-1}(3/\sqrt{2})$ (view from positive new y axis). The elastic coefficients thus obtained, along with those for the Iso (001) and GaAs (001), are listed below: nonzero elastic coefficients of Iso (001) ($\times 10^9$ N/m^2),

$$C_{11}=172.6;\quad C_{12}=53.8;\quad C_{44}=59.4; \tag{A1}$$

nonzero elastic coefficients of GaAs (001) ($\times 10^9$ N/m^2),

$$C_{11}=118.8;\quad C_{12}=53.8;\quad C_{44}=59.4; \tag{A2}$$

elastic coefficient matrix of GaAs (111),

$$\boldsymbol{C}=\begin{bmatrix} 145 & 45 & 36 & 0 & 12.73 & 0 \\ 45 & 145 & 36 & 0 & -12.73 & 0 \\ 36 & 36 & 154 & 0 & 0 & 0 \\ 0 & 0 & 0 & 41 & 0 & -12.73 \\ 12.73 & -12.73 & 0 & 0 & 41 & 0 \\ 0 & 0 & 0 & -12.73 & 0 & 50 \end{bmatrix} \times 10^9 \quad \text{N/m}^2; \tag{A3}$$

elastic coefficient matrix of GaAs (113),

$$\boldsymbol{C}=\begin{bmatrix} 152.81 & 31.79 & 41.79 & 0 & -4.72 & 0 \\ 31.79 & 145.7 & 48.91 & 0 & -10.38 & 0 \\ 41.79 & 48.91 & 135.70 & 0 & 15.09 & 0 \\ 0 & 0 & 0 & 54.51 & 0 & -10.38 \\ -4.72 & -10.38 & 15.09 & 0 & 47.39 & 0 \\ 0 & 0 & 0 & -10.38 & 0 & 37.39 \end{bmatrix} \times 10^9 \quad \text{N/m}^2. \tag{A4}$$

[1] D. Bimberg, M. Grundmann, and N. N. Ledentsov, *Quantum Dot Heterostructures* (Wiley, New York, NY, 1999).
[2] D. Leonard, M. Krishnamurthy, C. M. Reaves, S. P. Denbaars, and P. M. Petroff, Appl. Phys. Lett. **63**, 3203 (1993).
[3] J. M. Moison, F. Houzay, F. Barthe, L. Leprince, E. André, and O. Vatel, Appl. Phys. Lett. **64**, 196 (1994).
[4] Y. W. Zhang, A. F. Bower, and P. Liu, Thin Solid Films **424**, 9 (2003).
[5] J. Tersoff, C. Teichert, and M. G. Lagally, Phys. Rev. Lett. **76**, 1675 (1996).
[6] F. Liu, S. E. Davenport, H. M. Evans, and M. G. Lagally, Phys. Rev. Lett. **82**, 2528 (1999).
[7] T. Lippen, R. Nötzel, G. J. Hamhuis, and J. H. Wolter, J. Appl. Phys. **97**, 044301 (2005).
[8] G. Fasching and K. Unterrainer, Appl. Phys. Lett. **86**, 063111 (2005).
[9] Y. Temko, T. Suzuki, M. C. Xu, K. Pötschke, D. Bimberg, and K. Jacobi1, Phys. Rev. B **71**, 045336 (2005).
[10] V. Holý, G. Springholz, M. Pinczolits, and G. Bauer, Phys. Rev. Lett. **83**, 356 (1999).
[11] I. Daruka, A.-L. Barabási, S. J. Zhou, T. C. Germann, P. S. Lomdahl, and A. R. Bishop, Phys. Rev. B **60**, R2150 (1999).
[12] C. Teichert, M. G. Lagally, L. J. Peticolas, J. C. Bean, and J. Tersoff, Phys. Rev. B **53**, 16334 (1996).
[13] Q. Xie, A. Madhukar, P. Chen, and N. P. Kobayashi, Phys. Rev. Lett. **75**, 2542 (1995).
[14] G. S. Solomon, J. A. Trezza, A. F. Marshall, and J. S. Harris, Phys. Rev. Lett. **76**, 952 (1996).
[15] W. Lee, J-M. Myoung, Y-H. Yoo, and H. Shin Solid State Commun. **132**, 135 (2004).
[16] S. S. Quek and G. R. Liu, Nanotechnology **14**, 752 (2003).
[17] G. Springholz *et al.*, Mater. Sci. Eng., B **88**, 143 (2002).
[18] D. Srivastava and B. J. Garrison, J. Chem. Phys. **95**, 6885 (1991).
[19] B. A. Joyce and D. D. Vvedensky, Mater. Sci. Eng., R. **46**, 127 (2004).
[20] D. Srivastava and B. J. Garrison, Phys. Rev. B **47**, 4464 (1993).
[21] M. Meixner, R. Kunert, and E. Schöll, Phys. Rev. B **67**, 195301 (2003).
[22] M. Meixner and E. Schöll, Phys. Rev. B **67**, 121202 (2003).
[23] S. Clarke, M. R. Wilby, and D. D. Vvedensky, Surf. Sci. **255**, 91 (1991).
[24] V. Le Thanh, Physica E (Amsterdam) **23**, 401 (2004).
[25] E. Pan, R. Zhu, and P. W. Chung, J. Nanoeng. Nanosyst. **218**, 71 (2004).
[26] E. Pan, J. Appl. Phys. **91**, 6379 (2002).
[27] E. Pan, J. Appl. Phys. **91**, 3785 (2002).

[28] H. Brune, K. Bromann, H. Röder, and K. Kern, Phys. Rev. B **52**, R14380 (1995).
[29] H. Brune, M. Giovannini, K. Bromann, and K. Kern, Nature (London) **394**, 451 (1998).
[30] E. Pan and B. Yang, J. Appl. Phys. **90**, 6190 (2001).
[31] F. Elsholz, M. Meixner, and E. Scholl, Nucl. Instrum. Methods Phys. Res. B **202**, 249 (2003).
[32] V. P. Zhdanov and B. Kasemo, Surf. Sci. **437**, 307 (1999).
[33] K. Jacobi, Prog. Surf. Sci. **71**, 185 (2003).
[34] J. F. Nye, *Physical Properties of Crystals* (Clarendon, Oxford, 1985).